ACTIVE MEDIA

Nonequivalent Yb³⁺ centres in $Y_{1-x}Yb_xAl_3(BO_3)_4$ laser crystals

K.N. Boldyrev, M.N. Popova, L.N. Bezmaternykh, M. Bettinelli

Abstract. **The absorption spectra of nonlinear laser crystals $Y_{1-x}Yb_xAl_3(BO_3)_4$ grown from bismuth – lithium – molybdate and potassium – molybdate solution – melts are comparatively studied by high-resolution Fourier spectroscopy. The differences observed in the fine structure of the absorption spectra are correlated with the variations in the solution – melt composition and in the concentrations of bismuth and molybdenum impurities in the crystals. It is shown that the concentration of the molybdenum impurity (the main factor hindering lasing in the UV spectral region) in the single crystals grown from the bismuth – lithium – molybdate solutions is more than an order of magnitude smaller than in the crystals grown using the potassium – molybdate solution – melt. The described method can be used for express analysis of the quality of UV laser crystals and for improving the solution – melt technologies of growth of laser crystals and crystals used for generation of the fourth harmonic of Nd : YAG laser radiation.**

1. Introduction

The noncentrosymmetric trigonal aluminum borate crystals with the structure of the natural mineral huntite doped with rare-earth (RE) ions have attracted attention as promising laser materials for a long time. These crystals are characterised by a high chemical and temperature stability, high mechanical strength, optical transparency in the range from UV to mid-IR wavelengths, and a high optical nonlinearity [1]. Due to the specific structure, in which the RE – oxygen prisms are isolated from each other, the luminescence of RE ions is only slightly quenched even in concentrated crystals. The $YAl_3(BO_3)_4$ (YAB) and $GdAl_3(BO_3)_4$ (GAB) crystals doped with Nd^{3+} ions were

K.N. Boldyrev, M.N. Popova Institute for Spectroscopy, Russian Academy of Sciences, ul. Fizicheskaya 5, 142190 Troitsk, Moscow region, Russia; e-mail: kn.boldyrev@gmail.com, popova@isan.troitsk.ru;
L.N. Bezmaternykh L.V. Kirensky Institute of Physics, Siberian Branch, Russian Academy of Sciences, Academgorodok 50, 660036 Krasnoyarsk, Russia;
M. Bettinelli Lab. Solid State Chemistry, DB, Univ. Verona and INSTM, UdR Verona, 37134 Verona, Italy

used to create compact and efficient lasers, including lasers with self-frequency doubling [2, 3]. The concentrated $NdAl_3(BO_3)_4$ crystal is promising for the development of minilasers [4].

Recently, much attention has been paid to another RE ion, Yb^{3+}, which has only two energy levels in the entire energy range up to the energies corresponding to the UV spectral region; these levels are the ground $^2F_{7/2}$ level and the excited $^2F_{5/2}$ level with an energy of about 10000 cm^{-1} (Fig. 1). This level structure allows one to avoid losses related to the absorption from the excited state and to the cross-relaxation. These ions can be pumped by inexpensive industrial diode lasers emitting at a wavelength of about 980 nm. In this case, one obtains a quasi-three-level laser with a slightly different pump and laser wavelengths, which
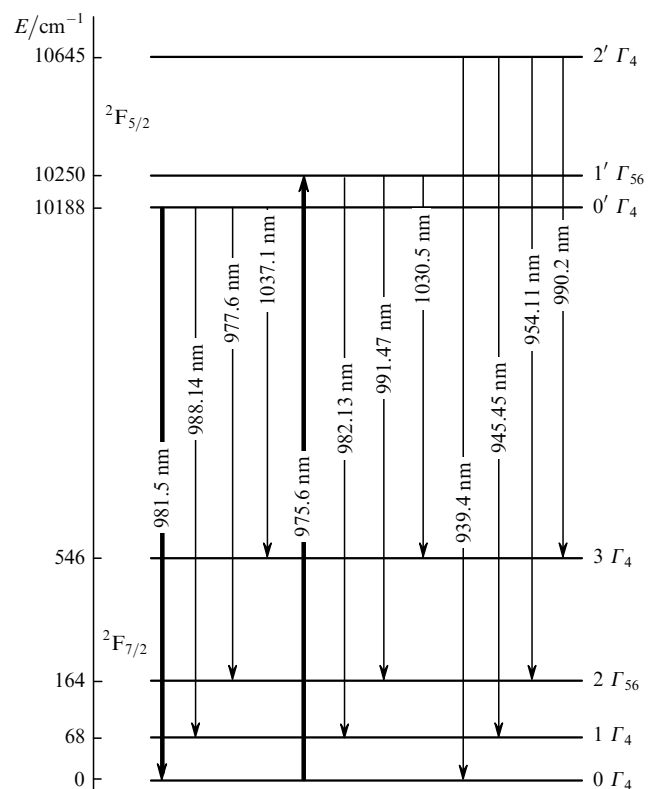
Figure 1. Energy level diagram of the Yb^{3+} ion. The energies and irreducible representations of levels are given for the $YbAl_3(BO_3)_4$ crystal according to work [5]. The bold arrows indicate the pump and laser transitions.

makes it possible to achieve a high efficiency and reduce the heating of the active medium by pump radiation.

Another important property of the ytterbium ion is the strong coupling of its electronic subsystem with lattice phonons (see, for example, [6]). Because of this, the electronic transition lines are strongly broadened, and the absorption and emission spectra show broad vibronic bands [6]. From the viewpoint of laser applications, the broad emission spectrum makes it possible to create lasers with ultrashort pulses and to tune the laser frequency within the vibronic band. The use of nonlinear media (in particular, aluminum borates) as matrices for Yb^{3+} ions allows one to shift the laser wavelength to the visible spectral region by frequency self-doubling and self-mixing. For example, in the Yb:YAl$_3$(BO$_3$)$_4$ crystal, cw laser radiation was obtained at a wavelength near 1040 nm [7], as well as in the green (513–546 nm) [8] and yellow (560–570 nm) [9] spectral regions.

Incongruently melting Y$_{1-x}$Yb$_x$Al$_3$(BO$_3$)$_4$ single crystals are grown from solution–melts that, along with the crystal-forming oxides, contain other components, such as, for example, potassium trimolybdate [1] or bismuth trimolybdate in combination with lithium molybdate [10]. This raises the important question of whether bismuth and molybdenum impurities can enter the crystal during crystallisation and how these impurities can affect the optical and laser properties of the grown single crystals. As was reported in [11], the molybdenum impurity is the main negative factor for generation of the fourth harmonic of Nd:YAG laser radiation and for UV lasing in YAB crystals.
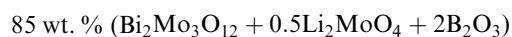
Previously [5], we found weak satellites of the 0–0 line of the $^2F_{7/2} \rightarrow {}^2F_{5/2}$ transition in the absorption spectrum of the YbAl$_3$(BO$_3$)$_4$ (YbAB) crystal and suggested that they are caused by transitions in Yb^{3+} ions whose nearest environment is perturbed by defects appeared due to the flux components entering the crystal. The present work is devoted to the study of defect formation in ytterbium-doped yttrium aluminum borates grown in two different laboratories using different fluxes. In particular, we managed to identify the spectral lines caused by defects present in the crystal due to molybdenum impurity. This result can be used for express analysis of the quality of UV laser crystals.

2. Experiment

The Y$_{1-x}$Yb$_x$Al$_3$(BO$_3$)$_4$ single crystals with different concentrations of ytterbium were grown on seeds from bismuth–lithium–molybdate solution–melts (which, in addition to the crystal-forming oxides Y$_2$O$_3$, Yb$_2$O$_3$, Al$_2$O$_3$ and B$_2$O$_3$, contained Bi$_2$O$_3$, Li$_2$O and MoO$_3$ oxides)

and from solution–melts based on potassium trimolybdate (which included K$_2$Mo$_3$O$_{10}$ in addition to the crystal-forming oxides). The former were grown at the Institute of Physics, Siberian Branch, Russian Academy of Sciences (Krasnoyarsk, Russia) and the latter were obtained at the University of Verona (Italy). The crystals studied in this work, as well as the notations of the used solution–melts are listed in Table 1.

The group of bismuth–lithium–molybdate solution–melts was based on a mixture of bismuth trimolybdate and lithium molybdate,

$$85 \text{ wt. } \% \text{ (Bi}_2\text{Mo}_3\text{O}_{12} + 0.5\text{Li}_2\text{MoO}_4 + 2\text{B}_2\text{O}_3)$$

$$+15 \text{ wt. } \% \text{ Y}_{1-x}\text{Yb}_x\text{Al}_3(\text{BO}_3)_4. \tag{1}$$

This solution–melt is denoted in Table 1 as Bi$_2$Mo$_3$O$_{12}$ (Nos 1–5). It was prepared by melting (at temperatures of 1000–1050 °C) a mixture of Bi$_2$O$_3$, MoO$_3$, Li$_2$CO$_3$, B$_2$O$_3$, Y$_2$O$_3$, Yb$_2$O$_3$, and Al$_2$O$_3$ powders in a proportion determined by the above formula. From this initial solution–melt, we grew on seeds single crystals No. 1 with $x = 0.07$, after which we added 0.05 Bi$_2$O$_3$ into the remaining solution–melt and performed one more crystallisation, thus growing single crystal No. 2. Then, we added 0.3 MoO$_3$ to the initial Bi$_2$Mo$_3$O$_{12}$ into the remaining solution–melt and, after crystallisation, obtained crystal No. 3. In Table 1, these solution–melts are denoted as Bi$_2$Mo$_3$O$_{12}$ + 0.05 Bi$_2$O$_3$ and Bi$_2$Mo$_3$O$_{12}$ + 0.15 MoO$_3$, respectively. On seeds, isomeric single crystals were grown with dimension up to 12–14 mm. A high optical quality was achieved at growth rates not exceeding 0.5 mm per day.

Single crystals Nos 6–8 were grown from solution–melts based on potassium trimolybdate by spontaneous crystallisation [12]. In these experiments, the initial reagents included, in addition to the crystal-forming oxides, K$_2$SO$_4$ and MoO$_3$, while the K$_2$Mo$_3$O$_{10}$ ingredient was formed as a result of the reaction

$$\text{K}_2\text{SO}_4 + 3\text{MoO}_3 = \text{K}_2\text{Mo}_3\text{O}_{10} + \text{SO}_3\uparrow.$$
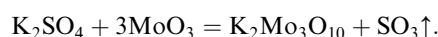
Therefore, we first melted the K$_2$SO$_4$ + 3MoO$_3$ mixture in a platinum crucible and then added the crystal-forming oxides so that their ratio to the melt was 40:60 wt. %. The proportions between the amounts of Y$_2$O$_3$, Yb$_2$O$_3$, and Al$_2$O$_3$ corresponded to the stoichiometric composition of Y$_{1-x}$Yb$_x$Al$_3$(BO$_3$)$_4$. The crucible covered by a platinum lid was returned to the furnace, heated to 1120 °C with a rate of 300 °C h^{-1}, kept at this temperature for three hours, and

Table 1. List of the studied samples and the used solution–melts (see the text). The relative concentration of YbII centres was estimated by the relative intensities of the satellite (frequency ~ 10200 cm^{-1}) and the main electronic line $^2F_{7/2}(0) \rightarrow {}^2F_{5/2}(0)$ of the Yb^{3+} ion.

No.	Sample	Solution–melt composition	Relative concentration of YbII centres (%)
1	YAl$_3$(BO$_3$)$_4$:Yb (7 %)	Bi$_2$Mo$_3$O$_{12}$	< 0.01
2	YAl$_3$(BO$_3$)$_4$:Yb (7 %)	Bi$_2$Mo$_3$O$_{12}$ + 0.05Bi$_2$O$_3$	< 0.01
3	YAl$_3$(BO$_3$)$_4$:Yb (7 %)	Bi$_2$Mo$_3$O$_{12}$ + 0.15MoO$_3$	< 0.8
4	YAl$_3$(BO$_3$)$_4$:Yb (10 %), Tm (5 %)	Bi$_2$Mo$_3$O$_{12}$	< 0.1
5	YbAl$_3$(BO$_3$)$_4$	Bi$_2$Mo$_3$O$_{12}$	$\ll 1.4$
6	YAl$_3$(BO$_3$)$_4$:Yb (0.3 %)	K$_2$Mo$_3$O$_{10}$	1.6
7	YAl$_3$(BO$_3$)$_4$:Yb (2.5 %)	K$_2$Mo$_3$O$_{10}$	3.2
8	YAl$_3$(BO$_3$)$_4$:Yb (8 %)	K$_2$Mo$_3$O$_{10}$	< 6.5

then cooled to 850 °C with a rate of 1 °C h^{-1}. To detach the crystals from the solution–melt, the crucible charge was boiled in concentrated KOH. The largest (5 × 6 mm) crystals contained solution–melt inclusions. Clear and transparent crystals with sizes up to 2 mm were used for optical measurements.

The absorption spectra of $Y_{1-x}Yb_xAl_3(BO_3)_4$ single crystals for the σ-polarised light ($k \perp c$, $E \perp c$, and k, E are the wave-vector and the strength of the probing radiation field and c is the crystallographic axis) were measured at a temperature of 3.5 K in the region of the $^2F_{7/2} \rightarrow {}^2F_{5/2}$ transition of the Yb^{3+} ion with a spectral resolution up to 0.1 cm^{-1}. The measurements were performed using a high-resolution (up to 0.1 cm^{-1}) Bruker IFS 125 HR Fourier spectrometer with a silicon detector and a Cryomech ST403 closed-cycle cryostat. As a polariser, we used a Glan–Taylor prism.

The elemental composition of the samples was controlled by optical emission spectroscopy (OES) using a Papuas 4DI OES spectrometer (spectral range 240–410 nm, spectral resolution 0.09 nm) designed and fabricated at the Institute of Spectroscopy, Russian Academy of Sciences. A sample was ground into powder, mixed with pure carbon (graphite), and placed between the spectrometer electrodes. This allowed us to observe the spectral lines of the sample atoms in the electric arc passing through the sample. Important drawbacks of this method are that the amount of impurities is difficult to determine due to the nonlinear dependences of the impurity line intensities on the impurity concentrations and that the detection sensitivity is different for different atoms (the lighter the atom, the weaker its line intensity). Despite these drawbacks, normalising an impurity line intensity to the line intensity of an atom whose concentration is known, one can obtain information on the relative concentrations of this impurity in different samples.

Figure 2 shows the optical emission spectra of yttrium aluminum borate crystals grown using different fluxes. One can see from Fig. 2 that the bismuth concentration in the crystal with an excess of MoO_3 is smaller than in the crystal with an excess of Bi_2O_3 and, naturally, the Bi line is completely absent in the crystals grown with the $K_2Mo_3O_{10}$ flux. Figure 2b clearly shows the molybdenum lines in the Yb : YAB crystal grown with the $K_2Mo_3O_{10}$ flux. These lines are absent in the other compounds, even in the crystal grown using the $Bi_2Mo_3O_{12}$ flux with an excess of MoO_3, which, probably, is caused by a low sensitivity of the OES method to the molybdenum ion.

3. Results and discussion

Figure 3 shows the low-temperature absorption spectra of different aluminum borates for the σ-polarised light. The effective absorption cross section of Yb^{3+} ions

$$\sigma = \alpha / n_{Yb}$$

allows one to compare the spectra of aluminum borates with different ytterbium concentrations (here α is the absorption coefficient and n_{Yb} is the concentration of ytterbium ions). The shape of the spectra only slightly depends on the ytterbium concentration and resembles the spectra of Yb : YAB (0.3 %–9 %) [13] and YbAB [5]
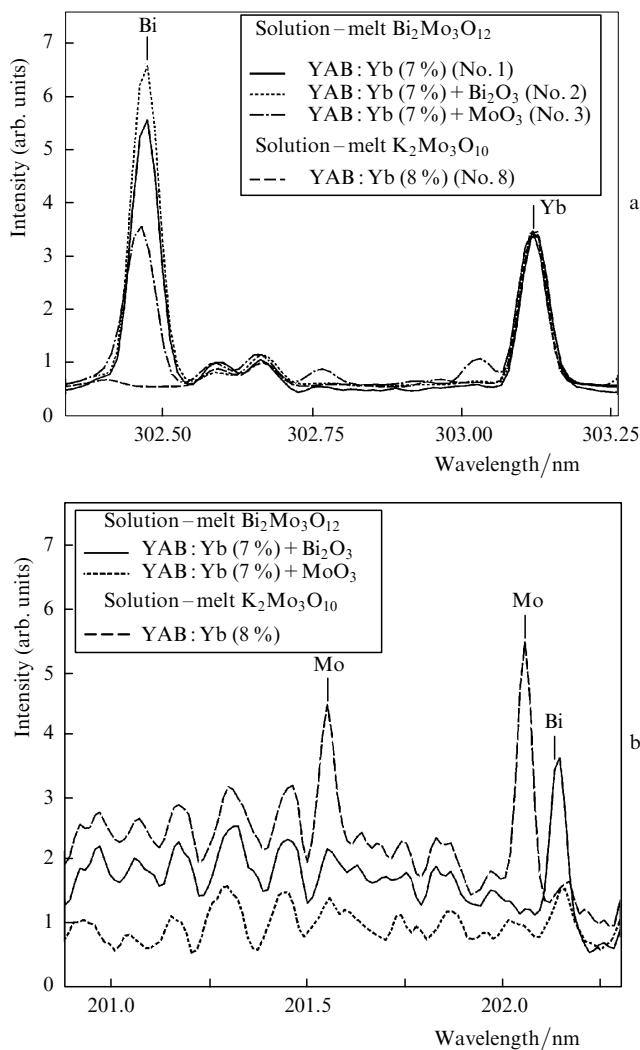

Figure 2. Atomic emission spectra of yttrium aluminum borates grown with different fluxes in the regions of 301–303 (analysis of bismuth and ytterbium impurities) (a) and 201–203 nm (analysis of molybdenum and bismuth impurities) (b).
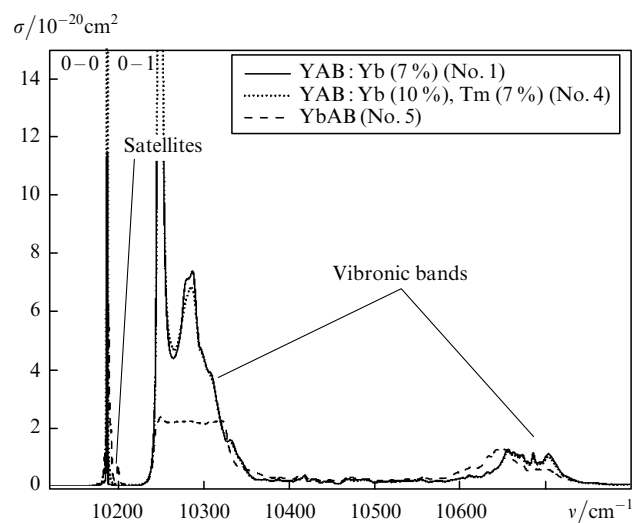
Figure 3. Absorption spectra of different ytterbium-doped aluminum borates.

crystals. On the high-frequency side of the purely electronic zero-phonon lines 0−0, 0−1, and 0−2 (see Fig. 2), one observes a vibronic structure caused by the interaction of ytterbium electronic levels with vibrations of the aluminum borate crystal lattice.

The spectra of all the studied crystals, as well as the spectrum of the previously studied YbAB crystal [5], show a series of narrow lines near the main electronic line 0−0. The satellites of the 0−0 line in the spectra of different ytterbium-doped yttrium aluminum borates are shown in Fig. 4 on an enlarged scale. In [5], we suggested that these lines belong to the absorption of Yb^{3+} ions whose nearest environment contains defect centres. In the process of crystallisation, some components of the solution can occupy the positions of ions in the crystal lattice of yttrium aluminum borates. Comparing the ionic radii of the RE [$r(Y^{3+}) = 0.90$ Å, $r(Yb^{3+}) = 0.87$ Å] and aluminum [$r(Al^{3+}) = 0.57$ Å] ions with the ionic radii of bismuth [$r(Bi^{3+}) = 1.02$ Å] and molybdenum [$r(Mo^{3+}) = 0.67$ Å], we supposed that bismuth can occupy the positions of RE ions and molybdenum can occupy the aluminum position [5]. This defect causes a local deformation of the crystal lattice and thus leads to a shift of the spectral lines of the closest Yb^{3+} ions (and to an inhomogeneous broadening of the lines of more distant ions). We also cannot rule out a heterovalent substitution, for example, the substitution of aluminum by the Mo^{5+} ion with a local charge compensation due to K$^+$ or Li$^+$ impurities in the positions of RE ions.
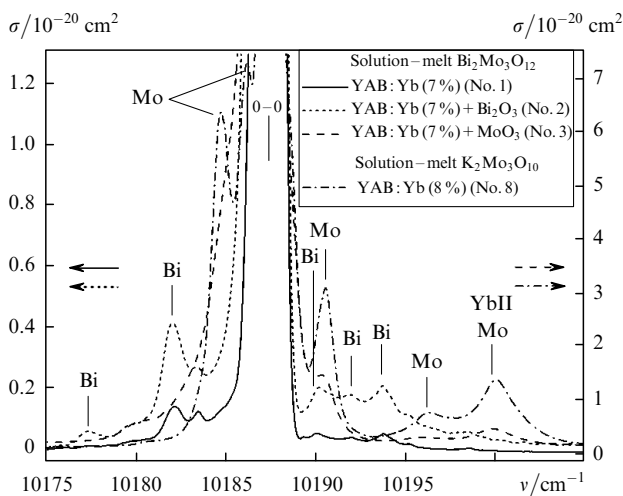
Figure 4. Absorption spectra in the region of the $^2F_{7/2}(0) \rightarrow {}^2F_{5/2}(0)$ transition in yttrium aluminum borates doped with Yb^{3+} ions with similar concentrations but grown using different fluxes. The ordinate scales are significantly different for samples 1, 2 and 3, 8.

Our comparison of the absorption spectra of the crystals grown with different fluxes (Fig. 4) shows that the integral intensity of satellites in the case of fluxes based on Bi$_2$Mo$_3$O$_{12}$ is considerably lower than for the flux based on K$_2$Mo$_3$O$_{10}$. In the first case, Bi$_2$O$_3$ is more soluble in the molybdate flux, which reduces the formation of the mentioned substitutional defects. The comparison of the spectra of crystals grown using the flux based on Bi$_2$Mo$_3$O$_{12}$ with an excess of bismuth with the spectra of crystals grown with the same flux but with an excess of molybdenum allowed us to

precisely determine which defects are responsible for some or other satellites. In particular, the previously observed YbII centre with the 0−0 line frequency near 10200 cm^{-1} [13, 5] can be reliably identified as the Yb^{3+} ion in a regular lattice site whose nearest environment contains a defect in the form of a molybdenum ion. At the same time, the analysis of the spectra of crystals grown with the K$_2$Mo$_3$O$_{10}$ flux (the dot-and-dash curve in Fig. 4) points to a considerable concentration of molybdenum in these crystals.

Summary Table 1 shows the integral intensity of the YbII centre line with respect to the main 0−0 transition line for the studied crystals. This quantity is equal to the relative concentration of YbII centres and is considerably higher in the crystals grown with the K$_2$Mo$_3$O$_{10}$ flux. The sign '<' in Table 1 means that the main 0−0 line is saturated and the given value is the upper estimate of the relative concentration of YbII centres. The sign '≪' used in Table 1 in the case of YbAl$_3$(BO$_3$)$_4$ indicates that the main line is strongly saturated and the real relative concentration for this sample is considerably smaller than the given value. Note that the compound grown with the bismuth–molybdate flux using the calculation formula corresponding to the crystal stoichiometry, nevertheless, contains bismuth (see Fig. 4). This occurs because the high volatility of MoO$_3$ does not allow one to avoid losses of this component during melting and successive homogenisation of the solution–melt, and as a result the final composition has some excess of Bi$_2$O$_3$ over the Bi$_2$Mo$_3$O$_{12}$ stoichiometry.

Finally, note that our investigation of the fine structure of the zero-phonon 0−0 line of the Yb^{3+} ion in the YAB crystal allowed us to detect the flux impurities contained in the crystal in very small concentrations, which could not be detected by optical emission spectroscopy.

4. Conclusions

(i) It is shown that the satellite lines near the optical absorption line $0({}^2F_{7/2}) - 0({}^2F_{5/2})$ in the Yb^{3+} ion in Y$_{1-x}$Yb$_x$Al$_3$(BO$_3$)$_4$ ($0.03 \leqslant x \leqslant 1.0$) single crystals are caused by transitions in the Yb^{3+} ions neighbouring the Bi^{3+} and Mo^{3+} impurity ions. The Yb^{3+}(Mo) and Yb^{3+}(Bi) centres are separated.

(ii) The measurement of the fine structure of the zero-phonon lines of RE ions in aluminum borate crystals can be a sensitive method for detecting the impurities entering the crystal during the growth from a solution–melt. In particular, this method can be used for express analysis of harmful molybdenum impurities in UV laser crystals.

(iii) From the relative intensity of the satellite lines related to the molybdenum impurities, it is determined that the concentration of molybdenum in the Y$_{1-x}$Yb$_x$Al$_3$(BO$_3$)$_4$ crystals grown from potassium–molybdate solution–melts is more than 100-fold higher than in crystals grown from bismuth–lithium–molybdate solution–melts.

(iv) On the whole, the obtained data are of interest for the growth and characterisation of aluminum borate crystals that can be used in UV lasers, as well as for the improvement of the growth technology of rare-earth aluminum borate single crystals for development of different lasers.

References

1. Leonyuk N.I., Leonyuk L.I. *Progr. Cryst. Growth Charact.*, **31**, 179 (1995).
2. Jaque D. *J. All. Comp.,* **204**, 323 (2001).
3. Brenier A., Tu C., Zhu Z., Wu B. *Appl. Phys. Lett.*, **84**, 2034 (2004).
4. Chen X., Luo Z., Jaque D., Romero J.J., Garcia Solé J., Huang Y., Jiang A., Tu C. *J. Phys.: Condens. Matter*, **13**, 1171 (2001).
5. Popova M.N., Boldyrev K.N., Petit P.O., Viana B., Bezmaternykh L.N. *J. Phys.: Condens. Matter*, **20**, 45, 455210 (2008).
6. Perlin Yu.E., Kaminskii A.A., Enakii V.N., Vylegzhanin D.N. *Pis'ma Zh. Eksp. Teor. Fiz.*, **30** (7), 426 (1979).
7. Wang P., Dawes J., Dekker P., Piper J. *Opt. Commun.*, **174**, 467 (2000).
8. Jiang H., Li J., Wang J., Hu X-B., Liu H., Teng B., Zhang C-Q., Dekker P., Wang P. *J. Cryst. Growth*, **233**, 248 (2001).
9. Burns P., Dawes J., Dekker P., Piper J., Li J., Wang J. *Opt. Commun.*, **207**, 315 (2002).
10. Bezmaternykh L.N., Mashchenko V.G., Sokolova N.A., Temerov V.L. *J. Cryst. Growth*, **69**, 407 (1984).
11. Yu X., Yue Y., Yao J., Hua Z. *J. Cryst. Growth*, **312**, 4029 (2010).
12. Bartl M.H., Gatterer K., Cavalli E., Speghini A., Bettinelli M. *Spectrochim. Acta Pt A: Molec. Biomolec. Spectrosc.,* **57**, 1981 (2001).
13. Ramirez M., Bausa L., Jaque D., Cavalli E., Speghini A., Bettinelli M. *J. Phys.: Condens. Matter*, **15**, 7789 (2003).